Journal of Scientific & Industrial Research
Vol. 84, December 2025, pp. 1331-1340
DOI: 10.56042/jsir.v84i12.3990

Artificial Neural Network Based Design of Circuit Parameters of Quasi Switched Boost DC-AC Inverter

S. Devi* & R. Seyezhai

Renewable Energy Conversion Laboratory, Department of Electrical and Electronics Engineering,
Sri Sivasubramaniya Nadar College of Engineering, Kalavakkam 603 110, Tamil Nadu, India

Received 14 July 2023; revised 05 June 2024; accepted 05 January 2026

The impedance source inverters are greatly preferred for photovoltaic applications as they can boost the voltage. There are numerous numbers of impedance and quasi-impedance network topologies available. This paper proposes the design of a High Gain Switched Boost Quasi-Impedance Source Inverter (HG-SBqZSI) for photovoltaic applications. There exists a set of parameters that affect the performance of the inverter. Hence, a proper design of the inverter is vital. Some of the parameters that influence the performance of the inverter are shoot through duty ratio, capacitor voltage ripple, inductor ripple, modulation index etc. This paper discusses the design and optimisation of HG-SBqZSI using Neural Networks (NN). The neural network-based prediction is carried out using NN toolbox in MATLAB/SIMULINK. The shoot through Duty ratio (D) is predicted using NN and on proper selection of shoot- through duty ratio value, the values of impedance elements and the gain of the inverter is optimised depending on the application.

Keywords: Duty ratio, Inverter design, Optimisation, Ripple, Voltage gain

Introduction

In recent years, there has been a huge increase in the utilisation of renewable energy sources. Solar energy is among the most promising sources of renewable energy. The Photovoltaic (PV) cells are used to convert the light energy obtained from sun into electrical energy. In order to provide the AC loads, the Direct Current (DC) electrical energy produced by PV cells must be transformed into AC. Hence, an inverter is required to convert the DC to AC.

In the conventional Voltage Source Inverters (VSIs), the output voltage is always lesser than the input voltage. Since the input voltage in PV applications is low, it must be increased before supplying the load. As a result, the input of a traditional VSI needs a DC-DC converter interface. Both the system's cost and losses are increased by the additional converter. Therefore, the Impedance Source Inverter (ZSI) is preferred as the inverter has inherent boosting capability.[1] With this the number of stages of power conversion is reduced. ZSI suffers from discontinuous input current that increases the input current ripple, inrush current and voltage stress across capacitors.

In order to overcome these disadvantages, quasi ZSI (qZSI) is used.[2] In addition to eliminating the inverter's drawbacks, it also has, reduced voltage stress on components and shared ground for dc source and H - bridge.[3] In both ZSI and qZSI, the voltage Gain (G) of the inverter is dependent on the shoot through Duty cycle (D). For ZSI and qZSI using Sinusoidal Pulse Width Modulation ($SPWM$), the relationship between value of Modulation index (M) and D given as $M \leq 1 - D$. Therefore, increase in the value of D results in decreased M value. Also, as reduced value of M results in reduced spectral quality of output waveform, there exists a trade-off while choosing the M and D values and, this restricts the G value of both the topologies. Consequently, a number of modified ZSI and qZSI have been developed to increase the inverter's voltage gain by using switched capacitors and inductors, however, these featured more passive components, which increased inverter losses.[4–8] Hence, to achieve maximum voltage gain with minimum number of components, a switched boost qZSI is used in this work.

The switched boost qZSI is a modified qZSI with an additional switch.[9] This adds another state of operation to the already existing modes of operation of qZSI. The performance of the inverter greatly

*Author for Correspondence
E-mail: devis@ssn.edu.in

depends upon design of the impedance network. Conventionally, the design of inverter is manually computed using the design equations of the inverter. As the design equations consists of multiple dependencies, while computing the design values manually, certain parameters are assumed depending upon the application. Hence, only a specified set of design values are obtained and this does not guarantee the optimal performance of the inverter. The conventional design of the circuit parameters includes solving the design equations manually by considering desired conditions. This conventional approach doesn't ensure the value obtained is the optimal value as it doesn't consider multiple operating conditions. Designing the circuit parameters manually with different operating conditions is tiresome and is prone to human errors.

De Leon Aldaco *et al.* [10] proposed the metaheuristic algorithms applied for power converters. The study involves designing of the components with optimum value of its dimensions, rating, operating frequency etc. This study shows the computational efficiency and precision using the algorithms are higher than the classical optimisation methods that are generally complex. Li *et al.* [11] designed the circuit parameters using Artificial Intelligence (AI) to design a synchronous buck converter for electric vehicles. The design involves volume, voltage and current ripples constraints of passive components of the converter. By deploying AI, the parameters were successfully designed by satisfying the constraints. Bui *et al.* [12] achieved the optimal design of the converter using deep neural network based surrogate model. This approach involves estimation of design parameters and efficiency without simulation model. This approach is time saving and also, as effective as the design of parameters by simulating the circuit with different operating conditions. From these literatures, the Neural Network (NN) based optimisation approach is adopted inorder to optimise the performance of the inverter, the design values consisting of multiple dependencies.

A Feed Forward NN (FFNN) is used to predict the value of D in order maximise the value of G and minimise the ripple in the impedance network.[13,14] The NN is trained having the boost factor (B), capacitor voltage ripple (ΔV_C) and inductor current ripple (ΔI_L) as inputs and D as the output. Thus, using FFNN, the value of D is predicted corresponding to the values of B, ΔV_C and ΔI_L fed to the network. This yields a wide data set consisting of maximum combinations of the all the dependent variables. Hence, choosing the parameters from this data set ensures optimum performance of the inverter with enhanced gain. The simulation study of the proposed inverter with value of D obtained from the dataset is performed and the results are validated.

High Voltage Gain Switched Boost Quasi – Impedance Source Inverter (HG-SBqZSI)

The topology of HG-SBqZSI[9] has a H-bridge along with an impedance network consisting of a pair of inductors, capacitors and diodes with an additional switch as depicted by Fig. 1. There exist three operational states namely two Non-Shoot Through (NST) state and one Shoot Through (ST) state. The H-bridge's phase leg switches in NST1 are turned ON independently, and S_0 and D_1 are conducting and D_2 is turned off. Capacitors C_1 and inductor L_2 discharge in this state, while capacitor C_2 and inductor L_1 charge. Both the diodes D_1 and D_2 are conducting in NST2, discharging L_1 and L_2 and charging C_1 and C_2, with S_0 in off state. Only during the NST modes, S_0 in the impedance network is turned ON and in the ST mode, the switches in the H- bridge and diode D_2 conducts while diode D_1 is in off state.

Shoot - through Mode (ST)

In the ST mode, S_0 is turned off and D_1 is reverse biased. All the four switches ($S_1 - S_4$) of the H-bridge inverter is simultaneously turned ON and D_2 is forward biased. During this mode, the energy is stored in L_1 and L_2 and C_1 and C_2 gets discharged. The equivalent circuit depicting the ST mode of operation of HG-SBqZSI is given in Fig. 2(a).

Non-Shoot - through Mode - I (NST1)

In NST1, S_0 is turned ON and D_1 is forward biased. The switches of the H-bridge inverter are turned ON complementary and D_2 is reverse biased. This mode charges L_1 and C_2 while discharging C_1 and L_2. The equivalent circuit for NST1 of HG-SBqZSI is depicted by Fig. 2(b).

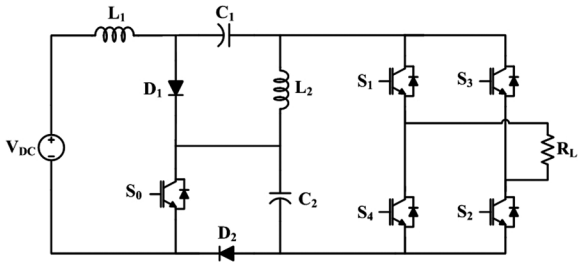

Fig. 1 — Topology of HG – SBqZSI

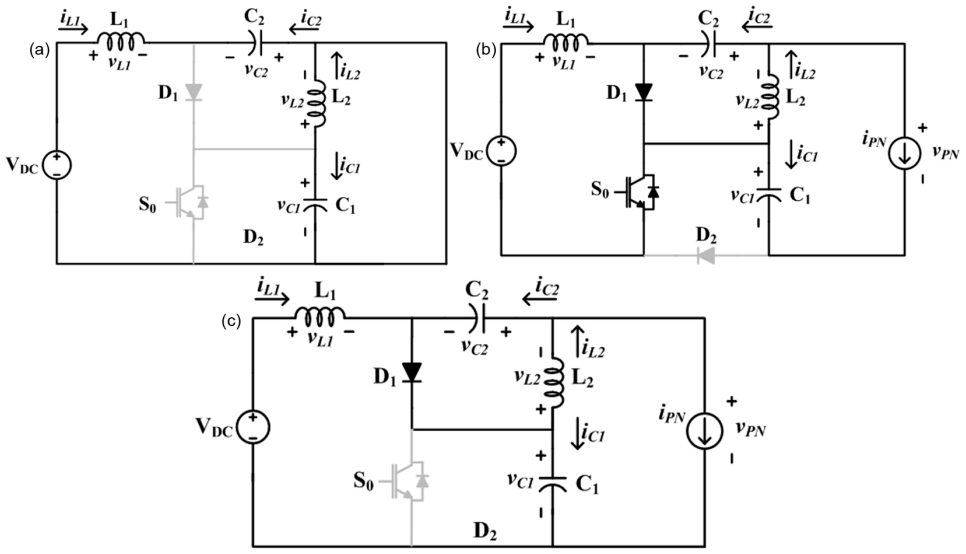

Fig. 2 — Operational modes of HG-SBqZSI: (a) ST mode, (b) NST1 and (c) NST2

Non-Shoot - through Mode - II (NST2)

During the NST2, S_0 is turned OFF and D_1 is forward biased. The H-bridge inverter supplies the load having D_2 is forward biased. This mode charges C_1 and C_2 while discharging L_1 and L_2. The equivalent circuit for NST2 of HG-SBqZSI can be seen in Fig. 2(c).

Selection of Design Parameters for HG-SBqZSI

Based on the modes of operation discussed in previous section, the steady state equations corresponding to the different modes of operation are given in Eqs (1) – (3).

$$\begin{cases} L_1 \dfrac{di_{L1}}{dt} = V_i + V_{C2} \\ L_2 \dfrac{di_{L2}}{dt} = V_{C1} \\ V_{PN} = 0 \end{cases} \quad and \quad \begin{cases} C_1 \dfrac{dv_{C1}}{dt} = -I_{L2} \\ C_2 \dfrac{dv_{C2}}{dt} = -I_{L1} \end{cases} \qquad \text{.... (1)}$$

$$\begin{cases} L_1 \dfrac{di_{L1}}{dt} = V_i \\ L_2 \dfrac{di_{L2}}{dt} = V_{C2} \\ V_{PN} = V_{C1} + V_{C2} \end{cases} \quad and \quad \begin{cases} C_1 \dfrac{dv_{C1}}{dt} = -I_{PN} \\ C_2 \dfrac{dv_{C2}}{dt} = I_{L2} - I_{PN} \end{cases} \qquad \text{.... (2)}$$

A modified sinusoidal PWM technique is used for HG-SBqZSI. The complementary pulses for $S_1 - S_4$ are generated using simple boost pulse width modulation by comparing V_{sine1} and V_{sine2} with V_{car1} and for S_0, it is generated separately by comparing $+V_{ref2}$ and $-V_{ref2}$ with V_{car2} having thrice the frequency of V_{car1}. The comparison of waveforms and the generation of pulses are shown in Fig. 3.

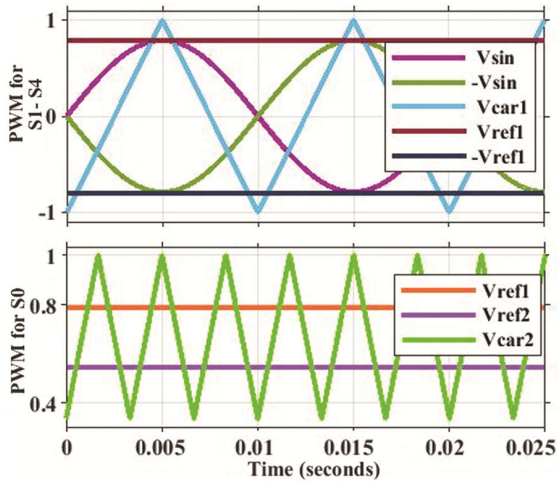

Fig. 3 — Modified PWM for HG-SBqZSI: (a) H-Bridge switches (b) S_0

$$\begin{cases} L_1 \dfrac{di_{L1}}{dt} = V_i - V_{C1} \\ L_2 \dfrac{di_{L2}}{dt} = -V_{C2} \\ V_{PN} = V_{C1} + V_{C2} \end{cases} \quad and \quad \begin{cases} C_1 \dfrac{dv_{C1}}{dt} = I_{L1} - I_{PN} \\ C_2 \dfrac{dv_{C2}}{dt} = I_{L2} - I_{PN} \end{cases} \qquad \text{.... (3)}$$

Using this modulation technique, the duration of ST mode is DT with NST1of $2DT$ and NST2 of

(*1 – 3DT*). By incorporating the time periods of each mode of operation, the value of *B* and *G* obtained are given in Eqs (4) and (5).

$$B = \frac{1}{1-4D+2D^2} \quad \text{... (4)}$$

$$G = \frac{1}{2M^2-1} \quad \text{... (5)}$$

From the Eqs (1) – (5), the inductances and capacitances values are calculated using the Eqs (6) – (9).[9]

$$L_1 = \frac{D(1-2D)(1-4D+2D^2)R_l}{2r_{L1}\% \times (1-D) \times f_s} \quad \text{... (6)}$$

$$L_2 = \frac{D(1-4D+2D^2)R_l}{2r_{L2}\% \times (1-D)(1-2D) \times f_s} \quad \text{... (7)}$$

$$C_1 = \frac{D(1-D)(1-2D)}{2r_{C1}\% \times (1-4D+2D^2) \times f_s R_l} \quad \text{... (8)}$$

$$C_2 = \frac{(1-D)^2}{2r_{C2}\% \times (1-4D+2D^2) \times f_s R_l} \quad \text{... (9)}$$

The *B* decides the *G* of the inverter and the design of the passive components of the inverter are dependent on the values of *D*, ripple, switching frequency (f_s) and load resistance (R_l) as shown in Eq. (4) and Eqs (6) – (9). The value of *L* and *C* is greatly influenced by the desired ripple in the inverter. As the value of *L* and *C* and, the values of ripple are inversely proportional to each other, the lower the value of ripple, the higher is the value of *L* and *C*. Also, with higher value of *L* and *C*, the size of the inverter becomes bulkier and results in poor power density. Therefore, the choice of the desired value of ripple is crucial in enhancing the performance and size of the inverter. As the dependence of *B*, capacitor voltage ripple (ΔV_c) and inductor current ripple (ΔI_L) on shoot through duty ratio (*D*) is evident from the Eq. (4) and Eqs (6) – (9), by optimising the *D*, the desired values of *B*, ΔV_C and ΔI_L is obtained. In order to reduce the computational complexity and establish a linear relationship between the above-mentioned variables, the f_s and R_l are assumed to be constants. Hence, the objective of the work proposed is to design the inverter with maximum boost along with minimum ripple values, by optimising the value of *D*. The values of *B*, ΔV_C and ΔI_L are depicted as a function of *D* in Fig 4.

From the Fig. 4, for *D* values from 0.2 to 0.3, the values of *B* are high and the ripple values ΔV_C and ΔI_L are low. Therefore, by finding the optimised value of *D*, it is possible to achieve high boost factor with minimised ripple values.

Design Optimisation using Neural Network

Based on the discussions from the previous section, the selection of *D* plays a vital role in deciding the performance of the inverter. There exists a huge change in the value of *B* for even small variation in *D*. Hence, to find the optimal value of *D*, with maximised boost factor and minimised ripple, an NN optimiser is required. As the NN-based optimisation necessitates extensive data training, data accessibility is vital to NN deployment. Through MATLAB programming, the Eqs (4) – (9) are solved to provide the data for the neural network's training. The values of *D*, *B*, and ripple are the only variables in the design equation; the other factors, including switching frequency and load resistance, are treated as constants. These presumptions are made in order to simplify computations and to build a linear relationship on desirable design parameters and NN optimisation is effective in solving such multi objective linear functions. There are three steps involved finding the optimum value of *D* using NN and is shown in Fig. 5.

For predicting the values of *D*, FFNN is used. In FFNN, the neurons of a layer have forward connections with neurons of the following layer. The back propagation, is way of adjusting weights of the epochs to minimise error.[15,16] For our application the structure of the FFNN is shown in Fig. 6.

Data Set Preparation

The data set required for the training was obtained by computing the values of *D* using the Eqs (4) – (9). The input vector consists of five rows, with *B*, ΔV_C and ΔI_L values. The output vector consists of corresponding *D* values. The sample input and output dataset are given in Tables 1 and 2.

Training

The network FFBPN is trained with the help MATLAB neural network tool box with the training parameters given in Table 3.

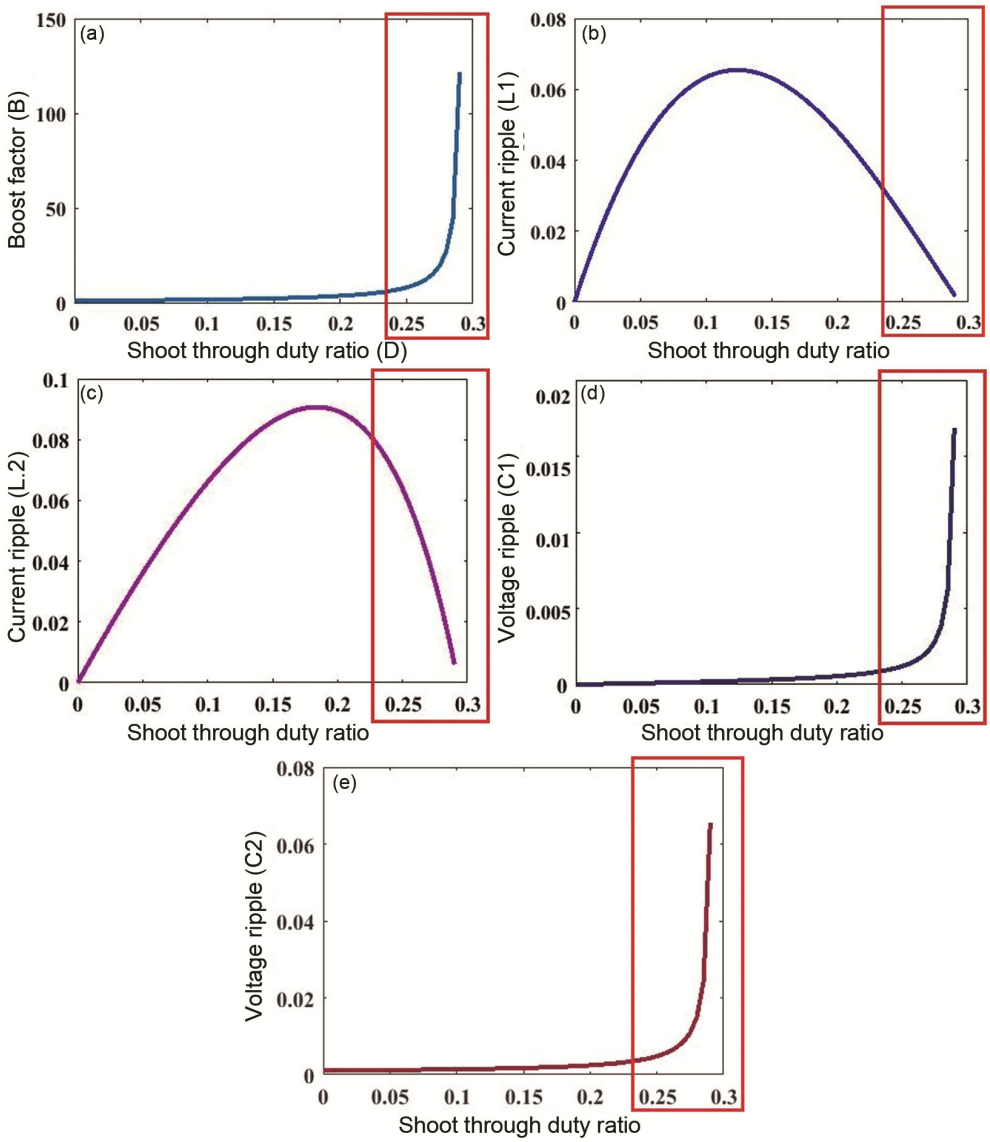

Fig. 4 — Dependence of performance parameters on *D:* (a) Dependence of *B* on *D*, (b) Dependence of ΔI_{L1} on *D*, (c) Dependence of ΔI_{L2} on *D*, (d) Dependence of ΔV_{C1} on *D* and (e) Dependence of ΔV_{C2} on *D*

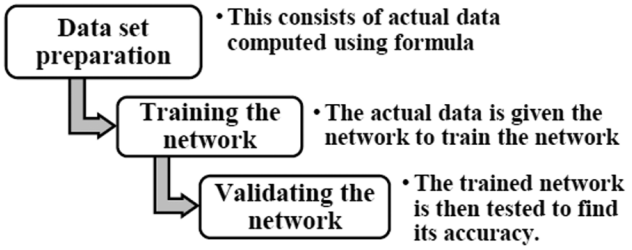

Fig. 5 — Steps involved in NN based prediction

The data prepared is fed as an input to the network. The accuracy of training is found by the validation graphs obtained at the end of the training. The validation graph thus obtained is shown in Fig. 7.

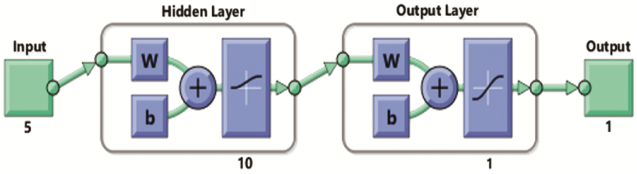

Fig. 6 — Feed forward neural network

From Fig. 7, the regression value obtained is 0.978 and the plot shows the fitting of data during the training of the network.

Effect of Training Parameters on the Network

The different training parameters used for creating the network are given in Table 3. The Table 4 gives

Table 1 — Sample of Input dataset for training the neural network

Parameters / Sample Nos.	Values of input dataset generated							
	1	2	3	4	5	6	7	8
B	1.882352	1.946282	2.014301	2.086811	2.164267	2.247191	2.336175	2.431906
ΔI_{L1}	0.065457	0.065335	0.065044	0.064591	0.063980	0.063216	0.062304	0.061249
ΔI_{L2}	0.077579	0.079541	0.081372	0.083065	0.084613	0.086008	0.087242	0.088306
ΔV_{C1}	0.000246	0.000260	0.000274	0.000289	0.000304	0.000320	0.000337	0.000355
ΔV_{C2}	0.001535	0.001569	0.001606	0.001644	0.001685	0.001730	0.001777	0.001828

Table 2 — Sample of Output dataset used for training the neural network

Parameters / Sample Nos.	Values of Output Dataset Generated							
	1	2	3	4	5	6	7	8
D	0.125	0.130	0.135	0.140	0.145	0.150	0.155	0.160

Table 3 — Parameters taken for training the neural network

Parameter	Value
Layers present	2
Hidden layer neuron count	10
Output layer neuron count	1
Transfer function for layer	Hyperbolic tangent sigmoid
Training function	Levenberg-Marquardt
Maximum epochs count	10000
Performance function	Mean squared error
Error target	0.00001
Rate of adaption	1.0
Back-propagation learning rate	0.1
Weights and bias used initially	Values generated randomly between 0 and 1

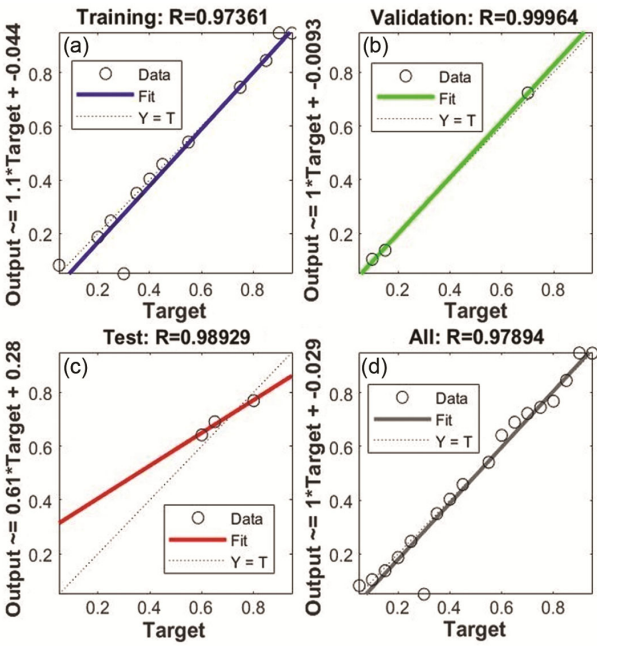

Fig. 7 — Validation graphs to assess the training of the NN: (a) Training (b) Validation (c) Test (d) All

the network's performance comparison for different training parameters.

From Table 4, for network with the training function: TRAINLM, activation function: LEARNGD and transfer function: LOGSIG, the regression value is obtained as 0.9999 as shown in Fig. 8 with least mean square error of 2.01E-9. This ensures the successful training of the network. Also, as the dependencies of the variables chosen for the network are linear, the training of the network is less complex and takes very less time for computation.

The NN is validated through the regression plot obtained after the completion of the training. The coefficient of correlation (R) depicts the closeness of the predicted and data with the actual data. As the value of R is close to unity, the predicted data is nearly same as the actual data used for training and validation and, this ensures successful training of the network.

Validation

While training the NN, the no. of data fed to the network plays a vital role in successful training of the network. The data required for training is generated using MATLAB programming. The identification of vital parameters, its correlation and dependencies are crucial before framing NN. The trained NN is fed with different sets of inputs and the results are verified to check for its robustness. The sample test case used to validate the NN is presented in Table 5 and Table 6 gives the comparison between actual and predicted values of *D* using NN.

From the Table 6, it is found that both the actual and predicted value of *D* using NN are in concurrence with each other and this ensures that the network is robust for prediction of *D*. Therefore, this trained NN

Table 4 — Performance comparison of network for different training parameters

Training function	Activation function	Transfer function	No. of neurons	Mean square error	Regression value	No. of iterations
TRAINLM	LEARNGD	TANSIG	10	2.71E-05	0.9993	12
		LOGSIG	10	2.01E-09	0.9999	99
		PURELN	10	6.8E-06	0.99955	24
	LEARNGDM	TANSIG	10	1.05E-07	0.99997	19
		LOGSIG	10	2.10E-09	0.9999	57
		PURELN	10	2.18E-05	0.997	11

Table 5 — Sample test case used for validation of NN

Parameters / Sample Nos.	Sample Test case values				
	1	2	3	4	5
B	1.242236	1.612903	2.247191	3.571429	8
ΔI_{L1}	0.043851	0.063378	0.063216	0.0483	0.023958
ΔI_{L2}	0.036092	0.066019	0.086008	0.089444	0.063889
ΔV_{C1}	8.49E-05	0.000186	0.000321	0.000548	0.001199
ΔV_{C2}	0.001195	0.001392	0.00173	0.002436	0.004795

Table 6 — Comparison of actual and predicted D values using trained NN

Parameters / Sample Nos.	Dataset values				
	1	2	3	4	5
D_{actual}	0.05	0.1	0.15	0.2	0.25
$D_{predicted}$	0.0500	0.1000	0.1500	0.2000	0.2500

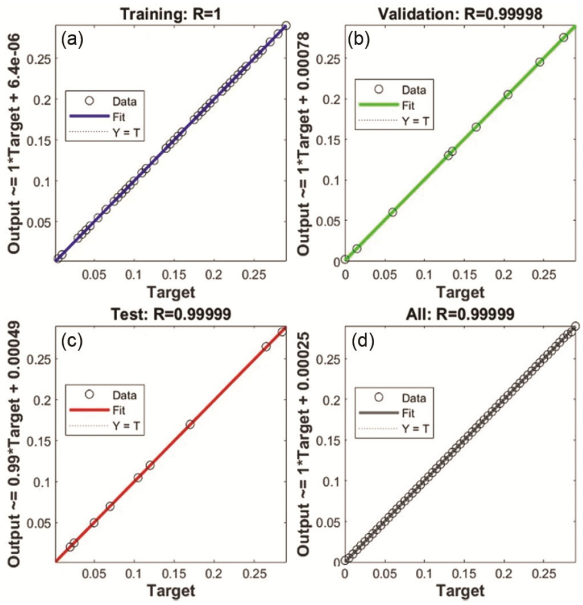

Fig. 8 — Regression plots obtained for network with the training function: TRAINLM, activation function: LEARNGD and transfer function: LOGSIG (a) Training (b) Validation (c) Test (d) All

is used to predict the value of D as per the requirement of the inverter.

The trained NN is fed with desired values of B, ΔI_{L1}, ΔI_{L2}, ΔV_{C1} and ΔV_{C2} to predict the required value of D and is given in Table 7.

Table 7 — Prediction of D values for desired values of B, ΔI_{L1}, ΔI_{L2}, ΔV_{C1} and ΔV_{C2}

Parameters	Values
B	*15*
ΔI_{L1}	0.01
ΔI_{L2}	0.05
ΔV_{C1}	0.002
ΔV_{C2}	0.01
D	0.271

From Table 7, for the D value is predicted to be 0.27 for maximised boost factor with minimised ripple as desired.

Simulation Study of HG – SBqZSI

From the value of D obtained using NN, simulation study was performed using MATLAB/Simulink and the simulation parameters computed using the Eqs (4) – (9) are given in Table 8.

Based on NN optimisation, the value of D obtained is 0.27 and hence, the modulation index is 0.73. The implementation of modified PWM is depicted in Fig. 9, where two separate carriers are used. One for the generation of gating pulse for H-bridge switches and the other for the active switch S_0.

The Fig. 10(a) depicts the load voltage waveform of HG-SBqZSI obtained through simulation for

D = 0.21 (using conventional design approach) and Fig. 10(b) depicts the load voltage waveform of HG-SBqZSI obtained through simulation for D = 0.27 (using NN optimisation). From Fig. 10, the peak output voltage obtained is 61V for D = 0.21 whereas for optimised value of D = 0.27, the peak output voltage obtained is 213V.

Performance Analysis of HG – SBqZSI

The comparison of voltage gains and rms value of output voltage obtained through conventional design approach and using NN optimisation is given in Table 9. From the Table 9, the G and output voltage value obtained using the NN optimisation is nearly three times the value obtained using conventional design approach.

The comparison of ripple values ΔV_{C1}, ΔV_{C2}, ΔI_{L1} and ΔI_{L2} using conventional design approach and NN optimisation are given in Table 10. From the Table 10, the ripple values obtained using NN optimisation is much lower when compared to conventional design approach.

Table 8 — Simulation parameters

Parameters	Values
Load power (W)	40
Source voltage (V)	19.25
Resistive load used (kΩ)	1
Carrier 1 - Frequency (kHz)	15
Carrier 2 - Frequency (kHz)	45
Shoot through duty ratio	0.27
Modulation Index	0.73
Impedance network	
Inductance L_1 (mH)	0.5
Inductance L_2 (mH)	1
Capacitance C_1 (μF)	2040
Capacitance C_2 (μF)	1360
Filter	
Inductance L_f (mH)	1
Capacitance C_f (μF)	470

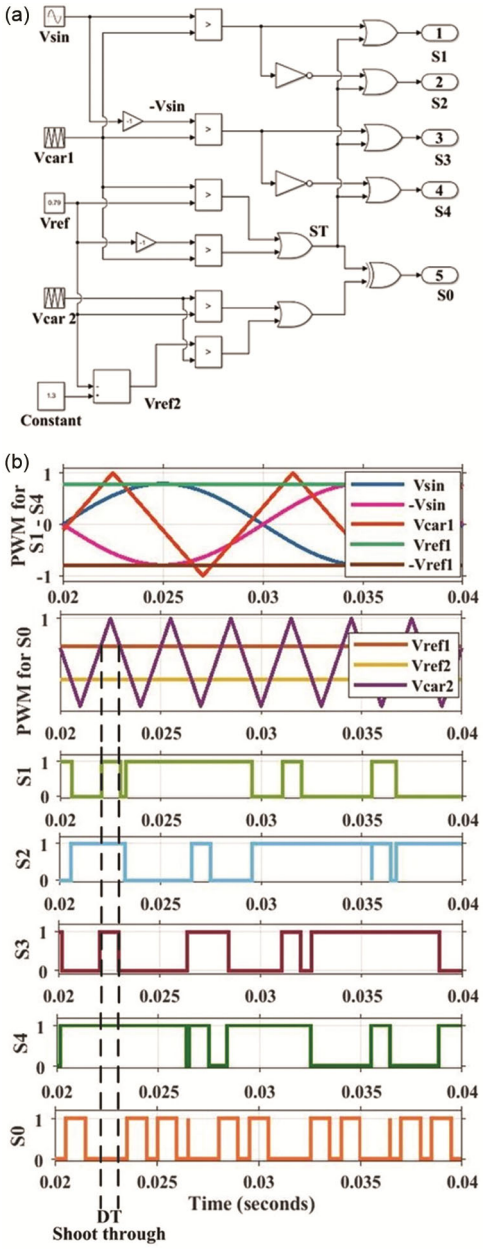

Fig. 9 — Modified PWM for HG – SBqZSI (a) Implementation of modified PWM for HG-SBqZSI and (b) Waveforms representation of modified PWM for HG-SBqZSI

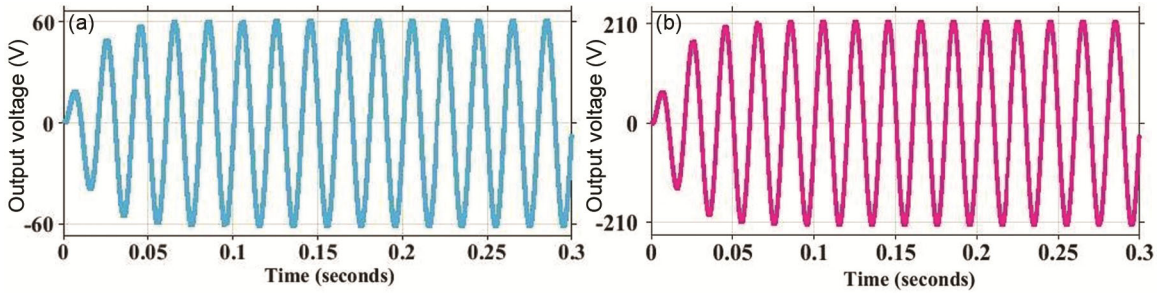

Fig. 10 — Output Waveforms of HG-SBqZSI: (a) for D = 0.21 conventional design approach and (b) for D = 0.27 using NN optimisation

Table 9 — Comparison of voltage gain and rms value of output voltage using conventional design approach and NN optimisation

Condition	Shoot through duty ratio	Voltage gain	RMS value of output voltage (V)
Conventional design approach	0.21	3.18	86
NN optimisation	0.27	11	301

Table 10 — Comparison of ripple values using conventional design approach and NN optimisation

Parameters	Values in Percentage (%)	
	Conventional design approach	NN optimisation
ΔI_{L1}	5	1
ΔI_{L2}	10	5
ΔV_{C1}	0.5	0.2
ΔV_{C2}	2	1

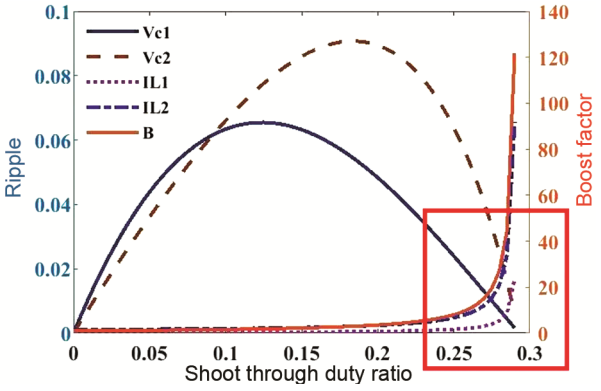

Fig. 11 — Expression of B, ΔV_{C1}, ΔV_{C2}, ΔI_{L1} and ΔI_{L2} as a function of D

From the Tables 9 and 10, the gain of the inverter is enhanced with reduction in the values of the ripple. This ensures that the objective of the design of the inverter is satisfied. By increasing the gain and reducing the ripple of the inverter, both the requirement of intermediate boost converter and the power quality issues of the inverter are mitigated. This ensures higher efficiency of the inverter. The dependence of B, ΔV_C and ΔI_L on D of HG-SBqZSI impedance network is shown in Fig. 11. From Fig. 11, for D values from 0.2 to 0.3, the corresponding value of B is high and the ripple values ΔV_C and ΔI_L are low. Therefore, this validates that the optimised value of D (= 0.27) obtained using NN, yields high boost factor with minimised ripple values in comparison with the conventional design approach.

However, while incorporating on the hardware systems, the data compatibility, interfacing of systems and computational and memory capacity of the existing systems are to be considered. Also, the parameters taken for study are specific to this topology and its application. Hence, the input parameters may vary for different topologies and their applications.

Conclusions

The NN based optimisation is ideal for finding optimum solutions for multiple dependent variables with less analytical computations and time saving. This paper presents NN based performance optimisation of HG-SBqZSI. The value of D influences the values of G, ΔV_{C1}, ΔV_{C2}, ΔI_{L1} and ΔI_{L2}. By optimising the value of D as 0.27 using NN-FFBPN, the value of G is enhanced to 11 along with the reduction in the ripple values of ΔV_{C1}, ΔV_{C2}, ΔI_{L1} and ΔI_{L2} to 0.04%, 0.25%, 0.04% and 0.07% respectively. Using MATLAB/Simulink, the performance parameters of the inverter designed conventionally and through NN optimisation are compared and the results obtained validates the prediction of NN. Thus, using NN for the selection of D optimises the performance of HG-SBqZSI for high gain and low ripple for photovoltaic applications. Similarly, this method shall be extended for other converter topologies for optimally sizing the passive components by suitably incorporating the design equations and the input-output constraints. By achieving optimal size of the components using the proposed method, the size of the power converter can be reduced, thereby increasing the power density of the converter. Hence, the NN based design of power converters can be applied for renewable energy conversion systems, electric vehicles and drives that employs high power density converters.

Conflict of Interest

The authors do not have any conflicts of interests to declare.

References

1 Peng F Z, Z-source inverter, in *IEEE Trans Ind Appl*, **39(2)** (2003) 504–510, https://doi.org/10.1109/TIA.2003.808920.

2 Anderson J & Peng F Z, A class of quasi-Z-source inverters, *2008 IEEE Ind Appl Soc Annu Meet* (Edmonton, AB, Canada), (2008) 1–7, https://doi.org/10.1109/08IAS.2008.301.

3 Anderson J & Peng F Z, Four quasi-Z-Source inverters, *2008 IEEE Power Elec Special Conf* (Rhodes, Greece), (2008) 2743–2749, https://doi.org/10.1109/PESC.2008.4592360.

4 Nguyen M K, Le T V, Park S J & Lim Y C, A Class of Quasi-Switched Boost Inverters, *IEEE Trans Ind Electron*, **62(3)** (2015) 1526–1536, https://doi.org/10.1109/TIE.2014.2341564.

5 Nguyen M K, Lim Y C & Park S J, A comparison between single-phase quasi- Z -source and quasi-switched boost inverters, *IEEE Trans Ind Electron*, **62(10)** (2015) 6336–6344, https://doi.org/10.1109/TIE.2015.2424201.

6 Ho A V, Yang S G, Chun T W & Lee H H, Topology of modified switched-capacitor Z-source inverters with improved boost capability, *2017 IEEE Appl Power Electron Conf Expo (APEC)* (Tampa, FL, USA), (2017) 685–689, https://doi.org/10.1109/APEC.2017.7930768.

7 Ahmad A, Bussa V K, Singh R K & Mahanty R, Switched-boost-modified Z-source inverter topologies with improved voltage gain capability, *IEEE J Emerg Sel Top Power Electron*, **6(4)** (2018) 2227–2244, https://doi.org/10.1109/JESTPE.2018.2823379.

8 Zhu X, Zhang B & Qiu D, A high boost active switched quasi-z-source inverter with low input current ripple, *IEEE Trans Ind Inf*, **15(9)** (2019) 5341–5354, https://doi.org/10.1109/TII.2019.2899937.

9 Nguyen M K, Duong T D, Lim Y C & Choi J H, High voltage gain quasi-switched boost inverters with low input current ripple, *IEEE Trans Ind Inf*, **15(9)** (2019) 4857–4866, https://doi.org/10.1109/TII.2018.2806933.

10 De Leon Aldaco S E, Calleja H & Aguayo Alquicira J, Metaheuristic optimization methods applied to power converters: A review, *IEEE Trans Power Electron*, **30(12)** (2015) 6791–6803, https://doi.org/10.1109/TPEL.2015.2397311.

11 Li X, Zhang X, Lin F & Blaabjerg F, Artificial-intelligence-based design for circuit parameters of power converters, *IEEE Trans Ind Electron*, **69(11)** (2022) 11144–11155, https://doi.org/10.1109/TIE.2021.3088377.

12 Bui V H, Chang F, Su W, Wang M, Murphey Y L & Da Silva F L, Deep neural network-based surrogate model for optimal component sizing of power converters using deep reinforcement learning, *IEEE Access*, **10** (2022) 78702–78712, https://doi.org/10.1109/ACCESS.2022.3194267.

13 Liao Y, Li Y, Chen M, Nordstrom L, Wang X & Mittal P, Neural network design for impedance modeling of power electronic systems based on latent features, *IEEE Trans Neural Netw Learn Syst*, **35(5)** (2024) 5968–5980, https://doi.org/10.1109/TNNLS.2023.3235806.

14 Karanayil B and Rahman M F, Artificial neural network applications, *Power Electronics Electric Drives Power Electronics Handbook*, Fourth Edition Elsevier, (2017) 1245–1260.

15 Hornik K, Approximation capabilities of multilayer Feedforward networks, *Neural Networks*, **4(2)** (1991) 251–257, https://doi.org/10.1016/0893-6080(91)90009-T.

16 Haykin S, Model building through regression in neural networks and learning machines, Third Edition Pearson, (2009), 68–89.